Int. J. Heat Mass Transfer. Vol. 27, No. 8, pp. 1337–1343, 1984
Printed in Great Britain

0017–9310/84 $3.00 + 0.00

MELTING OF SEMI-INFINITE REGION WITH VISCOUS HEATING

S. C. HUANG
Department of Mechanical Engineering, Southern University, Baton Rouge, LA 70813, U.S.A.

(*Received* 5 *July* 1983 *and in revised form* 9 *November* 1983)

Abstract—A closed-form solution is presented for the unsteady-state one-dimensional melting of semi-infinite solids on a hot moving wall. As a large shear stress is developed within the melt, viscous heating contributes greatly to the melting process and this effect is included in the analysis. Similarity technique and Green's function are applied to the governing equations and conditions. Calculations are performed for the melt with large Prandtl numbers to reveal the role of the viscous heating during transient melting.

NOMENCLATURE

Br	Brinkman number, $Ec\,Pr$
c	specific heat
D	constant, see equation (37)
Ec	Eckert number, $V_0^2/(c_1 T_m)$
erf	error function
f	function of ξ, see equation (30)
f_c	constant, see equation (31)
G	Green's function
k	thermal conductivity
L_m	latent heat of melting
Nu	Nusselt number, see equation (45)
q''	heat flux in the x-direction
Pr	Prandtl number of the melt, ν/α_1
s_1, s_2	functions of ξ, see equations (39) and (40)
Ste	Stefan number, $c_1 T_m/L_m$
t	time
T	temperature
u	velocity of the melt in the x-direction
v	velocity of the melt in the y-direction
V_0	constant velocity of the wall [m s^{-1}]
x	Cartesian coordinate perpendicular to the wall
y	Cartesian coordinate parallel to the wall
X	thickness of the melt.

Greek symbols

α	thermal diffusivity, $k/\rho c$
δ	delta function
η	similarity variable, see equation (16)
θ	dimensionless temperature, T/T_m
λ	melting parameter, see equation (15)
μ	viscosity of the melt
ν	kinematic viscosity of the melt, μ/ρ
ξ	similarity variable, see equation (20)
ρ	density
τ	shear stress.

Subscripts

1	liquid phase
2	solid phase
21	solid phase divided by liquid phase
i	for time $t < 0$
m	at the melting front $x = X$
0	at the wall $x = 0$.

INTRODUCTION

THE MELTING of solids on a hot moving surface occurs frequently in engineering systems. One typical example, among many others, is the melting of thermoplastics during extrusion. Because of the large shear stress developed within the thin melt, viscous heating is believed to be an important factor on the melting rate [1]. In spite of its wide applications, however, few analytical solutions are available.

For a semi-infinite flat plate, Pearson [2] proposed a steady-state two-dimensional (2-D) model. The non-Newtonian melt formed a thin layer of variable thickness in the neighborhood of the moving plate. Similarity solutions were obtained without calculation for several limiting cases under the zero pressure gradient assumption. Griffin [3] solved the same problem by using an integral energy-balance method. His numerical calculation agreed with the experimental results of Vermeulen [4] for low-density polyethylene. By using a shielding ratio, he found that the viscous heating can be predominant in the total energy added to the melt.

Grigorian [5] studied analytically the unsteady-state melting of semi-infinite solids adjacent to an adiabatic moving plate and the melting adjacent to a flowing semi-infinite fluid region. The latter case corresponds to the ballistic penetration in the atmosphere.

The purpose of this paper is to present a closed-form solution for the transient one-dimensional (1-D) problem where semi-infinite solids melt in contact with a hot infinite flat plate moving at constant speed. Without the relative motion between the plate and the melting solids, the problem is identical to the classical Stefan's problem [6]. The energy and momentum equations together with the relevant initial and boundary conditions are solved with the help of the similarity technique and Green's functions. Numerical calculations provide a better understanding of the role played by the viscous heating during the transient melting process.

FORMULATION OF THE PROBLEM

Consider the melting of solids in a semi-infinite region $0 < x < \infty$, $-\infty < y < \infty$ as shown in Fig. 1.

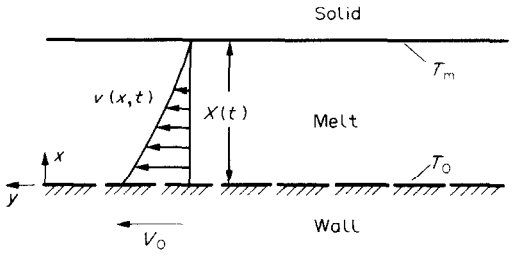

FIG. 1. Physical model of the problem.

Initially, the solid is at uniform temperature T_i below the melting temperature T_m. For time $t > 0$, a constant temperature T_0 higher than the melting temperature of the substance is maintained at the wall $x = 0$. In addition, the wall $x = 0$ is moved relative to the stationary solid with a constant speed $\pm V_0$ in the y-direction. Alternatively, the wall can be imagined to be stationary while the solid is moving parallel to the wall with constant speed $\mp V_0$. However, the former is preferred here. As a result of the combined effect of the applied excess wall temperature and the viscous dissipation due to the shear stress, the liquid phase is formed in the region $0 < x < X(t)$. To facilitate the analysis, the following assumptions are made.

(a) The unsteady-state process is 1-D, i.e. $u = u(x, t)$, $v = v(x, t)$, $T_1 = T_1(x, t)$, $T_2 = T_2(x, t)$, where notations are defined in the Nomenclature.

(b) The thermal and fluid properties such as density, thermal conductivity, viscosity, etc. are constant in each phase. But they may take different values in liquid and solid phases.

(c) The wall $x = 0$ is porous. This eliminates the pressure build-up caused by density change during melting.

(d) The pressure gradient along the y-direction is zero.

(e) The buoyancy-driven flow in the liquid phase due to nonuniform temperature distribution is negligible.

Consequently, the governing equations take the following forms

$$\frac{\partial u}{\partial x} = 0, \quad 0 < x < X(t), \quad t > 0, \tag{1}$$

$$\frac{\partial v}{\partial t} + u\frac{\partial v}{\partial x} = \nu\frac{\partial^2 v}{\partial x^2}, \quad 0 < x < X(t), \quad t > 0, \tag{2}$$

$$\frac{\partial T_1}{\partial t} + u\frac{\partial T_1}{\partial x} = \alpha_1\frac{\partial^2 T_1}{\partial x^2} + \frac{\nu}{c_1}\left(\frac{\partial v}{\partial x}\right)^2, \quad 0 < x < X(t), \quad t > 0, \tag{3}$$

$$\frac{\partial T_2}{\partial t} = \alpha_2\frac{\partial^2 T_2}{\partial x^2}, \quad X(t) < x < \infty, \quad t > 0. \tag{4}$$

The last term in equation (3) represents the heat generation due to the viscous heating in the liquid phase. One can see from the continuity equation (1) that the velocity u depends only on time. The mass balance at the phase change front requires that

$$u(t) = -(\rho_{21} - 1)\frac{dX(t)}{dt}, \quad t > 0. \tag{5}$$

In general, $\rho_{21} > 1$ and $u(t)$ is in the negative x-direction. According to the previous statement of the problem, the pertinent initial conditions are

$$v = 0, \qquad t = 0, \tag{6}$$

$$T_1 = T_2 = T_i, \qquad t = 0, \tag{7}$$

$$X = 0, \qquad t = 0, \tag{8}$$

and the boundary conditions are

$$v = \pm V_0, \quad x = 0, \quad t > 0, \tag{9}$$

$$T_1 = T_0, \quad x = 0, \quad t > 0, \tag{10}$$

$$T_2 = T_i, \quad x = \infty, \quad t > 0. \tag{11}$$

The conditions at the interface require that

$$v = 0, \quad x = X(t), \quad t > 0, \tag{12}$$

$$T_1 = T_2 = T_m, \quad x = X(t), \quad t > 0, \tag{13}$$

$$k_2\frac{\partial T_2}{\partial x} - k_1\frac{\partial T_1}{\partial x} = \rho_2 L_m\frac{dX(t)}{dt}, \quad x = X(t), \quad t > 0. \tag{14}$$

It is known that Stefan's problem is nonlinear in nature because of the unknown position of the interface. In addition, the thermal and fluid fields of the present problem are coupled. As the velocity field is confined in the melt region, its distribution depends on the rate of melting. The temperature distribution, on the other hand, depends on the velocity distribution caused by the viscous heating effect. The position of the phase front is in turn determined by the combined effect of the thermal and fluid flows. In the following, an analytical solution satisfying the system of equations (2)–(14) is sought.

ANALYSIS

Following the usual procedure of the similarity technique, the dimensionless constant λ and the similarity variable $\eta(x, t)$ can be defined as

$$\lambda = \frac{X(t)}{2(\alpha_1 t)^{1/2}}, \tag{15}$$

$$\eta = \frac{x}{X(t)} = \frac{x}{2\lambda(\alpha_1 t)^{1/2}}. \tag{16}$$

It is noticed that equation (15) satisfies the initial condition (8). The thickness of the melt increases with the square root of time. Substituting equations (15) and (16) into the governing equations (2)–(4), one obtains

$$-\xi\frac{dv}{d\xi} = \frac{Pr}{2\lambda^2}\frac{d^2 v}{d\xi^2}, \quad (\rho_{21} - 1) < \xi < \rho_{21}, \tag{17}$$

$$-\xi\frac{dT_1}{d\xi} = \frac{1}{2\lambda^2}\frac{d^2 T_1}{d\xi^2} + \frac{Pr}{2\lambda^2 c_1}\left(\frac{dv}{d\xi}\right)^2, \quad (\rho_{21} - 1) < \xi < \rho_{21}. \tag{18}$$

$$-\eta\frac{dT_2}{d\eta}=\frac{\alpha_{21}}{2\lambda^2}\frac{d^2T_2}{d\eta^2},\quad 1<\eta<\infty, \tag{19}$$

where

$$\xi=\eta+(\rho_{21}-1). \tag{20}$$

The similarity variable ξ is introduced for the melt region, i.e. $0<\eta<1$ or $\rho_{21}-1<\xi<\rho_{21}$, because of its repeated appearance. It is noticed that the factor Pr/λ^2 appears in both equations (17) and (18). The corresponding conditions (6), (7), (9)–(14) are transformed to

$$v=\pm V_0, \qquad \xi=\rho_{21}-1, \tag{21}$$

$$v=0, \qquad \xi=\rho_{21}, \tag{22}$$

$$T_1=T_0, \qquad \xi=\rho_{21}-1, \tag{23}$$

$$T_2=T_i, \qquad \eta=\infty, \tag{24}$$

$$T_1=T_2=T_m, \qquad \eta=1, \tag{25}$$

$$k_{21}\frac{dT_2}{d\eta}-\frac{dT_1}{d\eta}=2\rho_{21}T_m\lambda^2/Ste, \quad \eta=1. \tag{26}$$

The velocity profile v satisfying equations (17), (21) and (22) is easily found to be

$$v(\xi)=\pm V_0\frac{\operatorname{erf}(\lambda\rho_{21}/Pr^{1/2})-\operatorname{erf}(\lambda\xi/Pr^{1/2})}{\operatorname{erf}(\lambda\rho_{21}/Pr^{1/2})-\operatorname{erf}[\lambda(\rho_{21}-1)/Pr^{1/2}]}. \tag{27}$$

The solid temperature T_2 satisfying equations (19), (24) and (25) is simply

$$T_2(\eta)=T_i+(T_m-T_i)\frac{\operatorname{erfc}(\lambda\eta/\alpha_{21}^{1/2})}{\operatorname{erfc}(\lambda/\alpha_{21}^{1/2})}. \tag{28}$$

Both v and T_2 contain the melting parameter λ which has to be solved together with the temperature distribution in the melt.

Substituting equation (27) into equation (18), one obtains

$$\frac{d^2T_1}{d\xi^2}+2\lambda^2\xi\frac{dT_1}{d\xi}=-f(\xi)\,e^{-\lambda^2\xi^2}, \qquad (\rho_{21}-1)<\xi<\rho_{21}, \tag{29}$$

where

$$f(\xi)=f_cT_m\exp\left[-\left(\frac{2}{Pr}-1\right)\lambda^2\xi^2\right], \tag{30}$$

in which f_c is a constant defined by

$$f_c=\frac{4\lambda^2\,Ec}{\pi}\{\operatorname{erf}(\lambda\rho_{21}/Pr^{1/2})-\operatorname{erf}[\lambda(\rho_{21}-1)/Pr^{1/2}]\}^{-2}. \tag{31}$$

Multiplying both sides of equation (29) by $\exp(\lambda^2\xi^2)$, one obtains

$$\frac{d}{d\xi}\left(e^{\lambda^2\xi^2}\frac{dT_1}{d\xi}\right)=-f(\xi), \quad (\rho_{21}-1)<\xi<\rho_{21}. \tag{32}$$

It is noticed here that equation (32) is self-adjoint while equation (29) is not.

The Green's function $G(\xi|\xi')$ for the system of equations (32), (23) and (25) satisfies

$$\frac{\partial}{\partial\xi}\left(e^{\lambda^2\xi^2}\frac{\partial G}{\partial\xi}\right)=-\delta(\xi-\xi'), \quad (\rho_{21}-1)<\xi,\ \xi'<\rho_{21}, \tag{33}$$

and the following homogeneous boundary conditions

$$G=0 \quad \text{for} \quad \begin{cases}\xi=\rho_{21}-1 & \text{(34a)}\\ \xi=\rho_{21} & \text{(34b)}\end{cases} \qquad (\rho_{21}-1)<\xi'<\rho_{21}$$

The melt temperature distribution $T_1(\xi)$ is related to the Green's function by

$$T_1(\xi)=\int_{\rho_{21}-1}^{\rho_{21}}G(\xi|\xi')f(\xi')\,d\xi' + T_0\,e^{\lambda^2(\rho_{21}-1)^2}\frac{\partial G(\xi|\xi'=\rho_{21}-1)}{\partial\xi'} - T_m\,e^{\lambda^2\rho_{21}^2}\frac{\partial G(\xi|\xi'=\rho_{21})}{\partial\xi'}. \tag{35}$$

By omitting the intermediate steps, the Green's function satisfying equations (33) and (34) is found to be

$$G(\xi|\xi')=\frac{\pi^{1/2}}{2\lambda D}[\operatorname{erf}(\lambda\rho_{21})-\operatorname{erf}(\lambda\xi')]\times\{\operatorname{erf}(\lambda\xi)-\operatorname{erf}[\lambda(\rho_{21}-1)]\}, \quad \xi<\xi', \tag{36a}$$

$$G(\xi|\xi')=\frac{\pi^{1/2}}{2\lambda D}\{\operatorname{erf}(\lambda\xi')-\operatorname{erf}[\lambda(\rho_{21}-1)]\}\times[\operatorname{erf}(\lambda\rho_{21})-\operatorname{erf}(\lambda\xi)], \quad \xi'<\xi, \tag{36b}$$

where D is a constant defined by

$$D=\operatorname{erf}(\lambda\rho_{21})-\operatorname{erf}[\lambda(\rho_{21}-1)]. \tag{37}$$

Clearly $G(\xi|\xi')=G(\xi'|\xi)$ as is expected. Substituting equations (36a) and (36b) into equation (35), one obtains the following dimensionless result

$$\theta_1(\xi)=\frac{\pi^{1/2}f_c}{2\lambda D}\{[\operatorname{erf}(\lambda\rho_{21})-\operatorname{erf}(\lambda\xi)]s_1(\xi)+(\operatorname{erf}(\lambda\xi)-\operatorname{erf}[\lambda(\rho_{21}-1)])s_2(\xi)\}+\frac{\theta_0}{D}[\operatorname{erf}(\lambda\rho_{21})-\operatorname{erf}(\lambda\xi)]+\frac{1}{D}\{\operatorname{erf}(\lambda\xi)-\operatorname{erf}[\lambda(\rho_{21}-1)]\}, \tag{38}$$

in which $s_1(\xi)$ and $s_2(\xi)$ are functions of ξ defined by

$$s_1(\xi)=\int_{\rho_{21}-1}^{\xi}\{\operatorname{erf}(\lambda\xi')-\operatorname{erf}[\lambda(\rho_{21}-1)]\}\times\exp\left[-\left(\frac{2}{Pr}-1\right)\lambda^2\xi'^2\right]d\xi', \tag{39}$$

$$s_2(\xi)=\int_{\xi}^{\rho_{21}}[\operatorname{erf}(\lambda\rho_{21})-\operatorname{erf}(\lambda\xi')]\times\exp\left[-\left(\frac{2}{Pr}-1\right)\lambda^2\xi'^2\right]d\xi'. \tag{40}$$

The integrations in equations (39) and (40) cannot be carried out analytically. They can be evaluated by numerical quadrature.

It remains for only the unknown λ to be determined. Substituting equations (38)–(40) into equation (26) and keeping in mind that

$$s_2(\xi = \rho_{21}) = 0 \quad \text{and} \quad \frac{ds_2(\xi = \rho_{21})}{d\xi} = 0, \quad (41)$$

one obtains

$$\frac{f_c s_1(\rho_{21})}{D} e^{-\lambda^2 \rho_{21}^2} + \frac{2\lambda(\theta_0 - 1)}{\pi^{1/2} D} e^{-\lambda^2 \rho_{21}^2} - \frac{2\lambda k_{21}(1-\theta_i)}{(\pi\alpha_{21})^{1/2}} \frac{e^{-\lambda^2/\alpha_{21}}}{\operatorname{erfc}(\lambda/\alpha_{21}^{1/2})} = 2\rho_{21}\lambda^2/Ste. \quad (42)$$

If there is no relative motion between the wall and the melting solid, one can see that $f_c = 0$ and the first term of equation (42) can be dropped. It then reduces to the familiar Neumann's solution. If the initial temperature of the solid and the applied wall temperature are both at the melting temperature of the substance, i.e. $\theta_i = \theta_0 = 1$, the melting process is solely due to the viscous heating. In this case, equation (42) reduces to

$$\frac{V_0^2}{L_m} \frac{e^{-\lambda^2 \rho_{21}^2} s_1(\rho_{21})}{D\{\operatorname{erf}(\lambda\rho_{21}/Pr^{1/2}) - \operatorname{erf}[\lambda(\rho_{21}-1)/Pr^{1/2}]\}^2} = \frac{\pi}{2}\rho_{21}, \quad (43)$$

where $V_0^2/L_m = Ec\ Ste$. It is also noticed in equation (42) that λ is independent of the ratios k_{21} and α_{21} when $\theta_i = 1$, i.e. when the initial temperature is at the melting temperature.

With the above results, the heat flux at the wall $x = 0$ is given by

$$q_0'' = \frac{k_1 T_m e^{-\lambda^2(\rho_{21}-1)^2}}{(\pi\alpha_1 t)^{1/2} D} \times \left[(\theta_0 - 1) - \frac{\pi^{1/2} f_c}{2\lambda} s_2(\rho_{21} - 1)\right]. \quad (44)$$

The first term in the bracket of equation (44) corresponds to the applied excess temperature at the wall $x = 0$, while the second term corresponds to the viscous heating in the melt. It is noticed that they are opposite in sign. Thus the viscous dissipation generates a heat flux from the melt toward the moving wall. The corresponding Nusselt number is obtained from the above as

$$Nu = \frac{q_0'' X(t)}{k_1(T_0 - T_m)} = \frac{e^{-\lambda^2(\rho_{21}-1)^2}}{D} \times \left[\frac{2\lambda}{\pi^{1/2}} - \frac{f_c}{\theta_0 - 1} s_2(\rho_{21} - 1)\right], \quad (45)$$

which is a time-independent quantity. The Nusselt number is negative when the heat flux q_0'' is from the melt toward the wall. From equation (27), the shear stress at the wall $x = 0$ is given by

$$\tau_0 = \mp \frac{\mu V_0 e^{-\lambda^2(\rho_{21}-1)^2/Pr}}{(\pi\nu t)^{1/2}\{\operatorname{erf}(\lambda\rho_{21}/Pr^{1/2}) - \operatorname{erf}[\lambda(\rho_{21}-1)/Pr^{1/2}]\}}, \quad (46)$$

which is inversely proportional to the square root of time.

If the viscosity μ is a function of the temperature T_1, the obtained Green's function in equation (36) is still valid. In this case, however, integral equations are dealt with instead. A simple closed-form solution will not be possible.

RESULTS AND DISCUSSION

The rate of melting of the solid is proportional to the melting parameter λ. The values of λ can be determined numerically from the nonlinear algebraic equations (42) and (43) by the standard Newton's iteration method. In solving equation (42), seven dimensionless quantities, i.e. ρ_{21}, α_{21}, $k_{21}(1-\theta_i)$, θ_0, Pr, Ec, and Ste, have to be specified. As compared to the classical Neumann's solution, Pr and Ec are two additional parameters due to the added viscous heating effect. For the special case where $\theta_i = \theta_0 = 1$, the number of parameters reduces to three, i.e. ρ_{21}, Pr, and V_0^2/L_m, as can be seen from equation (43).

In many applications, the velocity of the hot wall is only moderate. The appreciable viscous heating mostly results from the large Prandtl number of the melting material. The reason is obvious by inspecting equation (18). Under the condition that $Pr \gg 1$, the constant f_c defined in equation (31) becomes the Brinkman number $Br = Pr\ Ec$. Consequently, the number of independent parameters in equation (42) is reduced by one as Pr and Ec are combined into a single parameter Br. For the special case where $\theta_i = \theta_0 = 1$, equation (43) reduces to

$$\frac{1}{2D}\left(Pr\frac{V_0^2}{L_m}\right) e^{-\lambda^2 \rho_{21}^2} s_1(\rho_{21}) = \rho_{21}\lambda^2, \quad (47)$$

in which $Pr(V_0^2/L_m) = Br\ Ste$. In addition, one can see from equation (17) that $dv/d\xi = \text{const.}$ when $Pr \gg 1$. Thus the heat generation term in equation (18) becomes a constant.

For the discussion that follows, a large Prandtl number of the melt will be assumed. Calculations are carried out for the six selected combinations of parameters listed in Table 1. For a better understanding of the order of magnitude of the dimensional quantities involved, one may take the low density polyethylene as an example. The relevant quantities are $T_m = 105°C$, $\rho_{21} = 1.18$, $Pr = 4.6 \times 10^7$, $Ste = 7.79$, and $Br =$

Table 1. Cases considered for numerical calculation: $\alpha_{21} = 1$ for all cases

Case	ρ_{21}	θ_0	$k_{21}(1-\theta_i)$	*Ste*
1	1.0	1.0	0.0	1.0
2	1.2	1.0	0.0	1.0
3	1.0	1.0	0.2	1.0
4	1.0	1.2	0.0	1.0
5	1.0	1.2	0.2	1.0
6	1.2	1.2	0.2	10.0

$41.95V_0^2$ [7]. These values correspond approximately to those of case 6. For this widely used polymer, one can see that $Br = 0.42$ is attainable by a moderate wall velocity of 0.1 m s^{-1}. Since the Brinkman number is proportional to the square of the wall velocity, an increase or decrease of V_0 may greatly change the *Br*-value.

Figure 2 shows the λ–*Br* relation for cases where $\theta_0 = 1$. As is expected, λ increases with the Brinkman number for all cases because of the increased viscous heating effect. It is noticed that the slopes decrease with increasing values of *Br*. This means that the change of Brinkman number has greatest impact on the melting rate when *Br* is small. Since $\theta_i = 1$ for both cases 1 and 2, λ depends on the product *Br Ste* for these two cases as is demonstrated in equation (47). Because of the choice of *Ste* = 1, one uses *Br* as the abscissa in place of $Pr(V_0^2/L_m)$. Thus Fig. 2 can also be interpreted by holding *Br* at a constant, say 0.1, and taking *Ste* as the abscissa from 1 to 11. The increase of λ with increasing *Ste* is easily explained as the result of the reduced fusion heat-sensible heat ratio.

For case 1, one can see that λ increases by about three times in the range of *Br* considered. Thus the important role of the viscous heating in the corresponding processes is established. Comparison of case 2 with case 1 shows that the volume expansion of the melt reduces

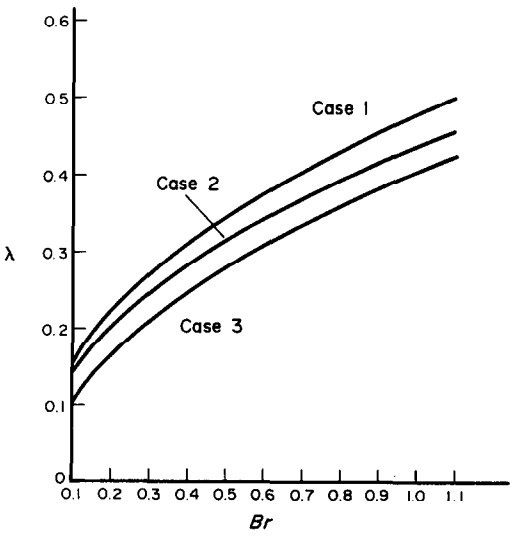

FIG. 2. λ–*Br* relation for cases with $\theta_0 = 1$.

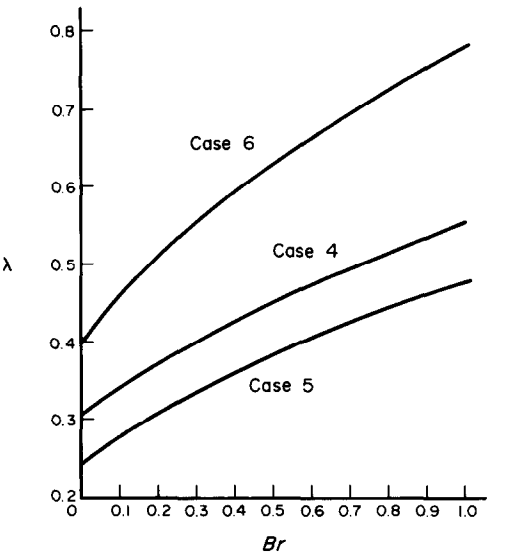

FIG. 3. λ–*Br* relation for cases with $\theta_0 = 1.2$.

the melting rate. This is because the resultant convection is in the opposite direction of the advancing phase front. The density effect is slight for small *Br* but is significant for large *Br*-values. For a given material, higher values of $k_{21}(1-\theta_i)$ means lower initial temperature. As more energy is needed in this case to bring the solid to its melting point, smaller λ-values are recorded for case 3.

Figure 3 shows the λ–*Br* relation for cases where $\theta_0 = 1.2$. Since the applied wall temperature is higher than the melting temperature of the solid, λ is nonzero at $Br = 0$. For $Br > 0$, one has the combined effect of wall heating and viscous heating. The increase of λ from that at $Br = 0$ is due to the viscous heating. As compared to the corresponding cases with $\theta_0 = 1$ in Fig. 2, one observes comparatively smaller slopes for both cases 4 and 5. The difference is most obvious in the small *Br*-region. This indicates that the raised wall temperature tends to reduce the effect of *Br* on the melting rate when the wall heating is dominant. As the fraction of viscous heating increases, the λ–*Br* relation behaves more and more like that of $\theta_0 = 1$. On the other hand, the role of the viscous heating seems to be greatly enhanced by a large Stefan number. Thus one can see for case 6 that the λ-value at $Br = 1$ is about twice that at $Br = 0$. Though a decrease of λ is expected for the increased ρ_{21} and $k_{21}(1-\theta_i)$, their effects are outweighed by the increase of λ associated with large Stefan number.

Figure 4 shows the temperature distribution in the melt for cases with $\theta_0 = 1$. It is found that the presented diagram can be equally applied to cases 1, 2, and 3 without modification. Hence the changes of ρ_{21} and θ_i have little effect on $\theta_1(\eta)$. This, however, does not imply that $\theta_1(x, t)$ is the same for these three cases. For example, case 2 has smaller values of λ and thus smaller regions of melt as compared to case 1 for a given time. Consequently, the high-temperature region is shifted

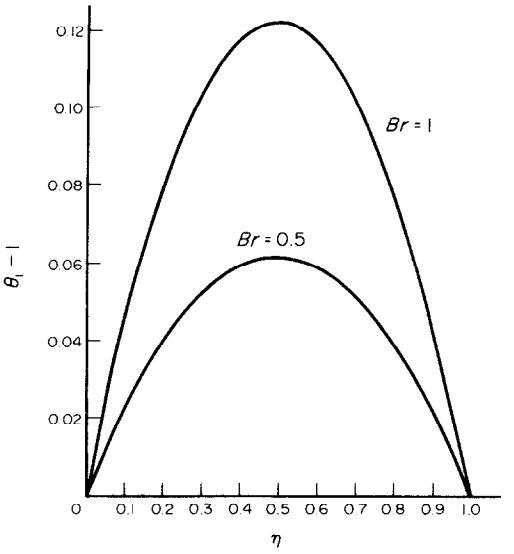

FIG. 4. Temperature distribution in the melt for cases with $\theta_0 = 1$.

toward the wall because of the expansion convection. The curves in Fig. 4 are approximately symmetric with respect to the center $\eta = 0.5$. The region close to the interface has a slightly lower temperature but is hardly noticeable. It is found from calculation that the maximum values of $\theta_1(\eta) - 1$ increase linearly with Brinkman number. The changes of the distribution $(\theta_1 - 1)/Br$ with different values of Br are very small for each case. Inspection of equation (38) does not reveal this fact.

Figure 5 shows the temperature distribution in the melt for case 6. The wall temperature is higher than the melting point in this case. For $Br = 0.1$, the curve is slightly convex from $\theta_1(\eta = 0) = 1.2$ to $\theta_1(\eta = 1) = 1$. As the Brinkman number is increased, the temperature

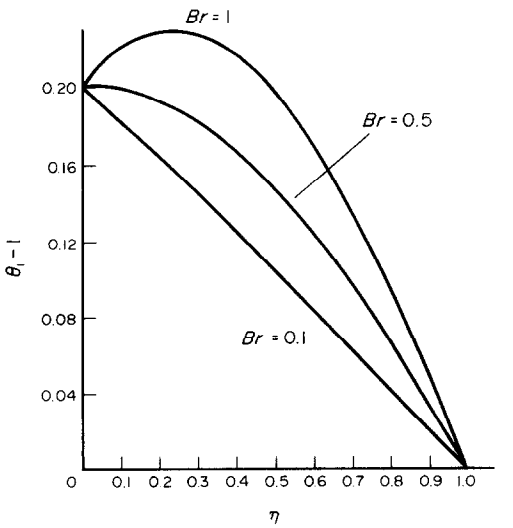

FIG. 5. Temperature distribution in the melt for case 6.

in the melt increases accordingly. When $Br = 0.5$, the slope at the wall is approximately zero. Thus the heat flux input to the melt due to the applied wall temperature is balanced by the heat flux output from the melt due to the viscous heating. As the Brinkman number is further increased, the second term in the bracket of equation (44) finally exceeds the first term and the net heat flux is from the melt to the moving wall. As is shown, the temperature near $\eta = 0$ is greater than the applied wall temperature for $Br = 1$. The maximum difference between the curves for $Br = 1$ and 0.1 occurs approximately at $\eta = 0.5$. For the same Br, the temperature distribution for case 5 is found to be slightly higher than that for case 6. Since the RHS of equation (26) decreases with increasing Stefan number, the heat flux of the melt at the interface for case 6 is smaller.

CONCLUSION

A closed-form solution is obtained for Stefan's problem with a moving hot wall. For large Prandtl numbers, one has the following results.

(a) The shear stress developed in the thin melt is large enough to significantly change the melting rate even at moderate wall speed. The important parameters are the Brinkman number and the Stefan number.

(b) The effect of the expansion convection on the melting rate increases with the Brinkman number.

(c) Raised wall temperature reduces the viscous heating effect on the melting rate.

(d) Materials with large Stefan numbers experience greater viscous heating effect.

(e) For cases where $\theta_0 = 1$, ρ_{21} and θ_i have little effect on the $\theta_1(\eta)$ distribution.

(f) Beyond the critical Brinkman number, the temperature in the melt can be greater than the applied wall temperature.

With additional effort, the solution can be extended to multiphase melting.

REFERENCES

1. J. T. Lindt, A dynamic melting model for a single screw extruder, *Polym. Engng Sci.* **16,** 284–291 (1976).
2. J. R. A. Pearson, On the melting of solids near a hot moving interface, with particular reference to beds of granular polymers, *Int. J. Heat Mass Transfer* **19,** 405–411 (1976).
3. O. M. Griffin, An integral energy-balance model for the melting of solids on a hot moving surface, with application to the transport processes during extrusion, *Int. J. Heat Mass Transfer* **20,** 675–683 (1977).
4. J. R. Vermeulen, Het smelten Van polymeerkorrels aan hete oppervlakken, Ph.D. thesis, Technische Hogeschool Delft (1970).
5. S. S. Grigorian, On heating and melting of a solid body owing to friction, *J. Appl. Math. Mech.* **5,** 815–825 (1958).
6. H. S. Carslaw and J. C. Jaeger, *Heat Conduction in Solids*, Chap. 11. Clarendon Press, London (1959).
7. J. R. Vermeulen, Ph. M. Gerson and W. J. Beek, The melting of a bed of polymer granules on a hot moving surface, *Chem. Engng Sci.* **26,** 1445–1455 (1971).

FUSION D'UNE REGION SEMI-INFINIE AVEC UN CHAUFFAGE VISQUEUX

Résumé—Une solution analytique est présentée pour la fusion variable monodimensionnelle de solides semi-infinis sur une paroi mobile et chaude. Comme une grande contrainte de cisaillement est développée dans le bain, le chauffage visqueux contribue fortement au mécanisme de fusion et cet effet est inclus dans l'analyse. Une technique de similitude et la fonction de Green sont appliquées aux équations et aux conditions. Des calculs sont conduits pour la fusion avec des nombres de Prandtl élevés pour montrer le rôle du chauffage visqueux pendant la fusion transitoire.

SCHMELZEN EINES HALBUNENDLICHEN GEBIETS MIT VISKOSEM ERWÄRMEN

Zusammenfassung—Es wird eine geschlossene Lösung für das instationäre eindimensionale Schmelzen eines halbunendlichen Festkörpers an einer heißen, bewegten Wand angegeben. Da eine große Scherkraft in der Schmelze entwicklet wird, trägt die viskose Erwärmung wesentlich zum Schmelzprozeß bei, was in den Berechnungen berücksichtigt wird. Es werden Ähnlichkeitsmethoden und die Green'sche Funktion auf die Bestimmungsgleichungen und Randbedingungen angewendet. Die Berechungen wurden für eine Schmelze mit großen Prandtl-Zahlen durchgeführt, um die Rolle der viskosen Erwärmung beim instationären Schmelzen zu beleuchten.

ПЛАВЛЕНИЕ ПОЛУБЕСКОНЕЧНОГО ТЕЛА НА НАГРЕТОЙ ДВИЖУЩЕЙСЯ СТЕНКЕ

Аннотация—Представлено решение в замкнутом виде для случая нестационарного одномерного плавления полубесконечных твердых тел на нагретой движущейся стенке. По мере возникновения при плавлении значительного касательного напряжения на процесс плавления начинает оказывать большое влияние нагрев из-за трения, что и анализируется в данной работе. Решение получено с помощью автомодельного метода и функции Грина. Расчеты выполнены для расплава с большими числами Прандтля.